Journal of Applied Sciences

ISSN 1812-5654

science alert

ANSInet
an open access publisher
http://ansinet.com

Journal of Applied Sciences 9 (23): 4099-4114, 2009
ISSN 1812-5654
© 2009 Asian Network for Scientific Information

Tectonic Zoning of Iran Based on Self-Organizing Map

[1]A. Zamani, [1]M. Nedaei and [2]R. Boostani
[1]Department of Earth Sciences, Faculty of Sciences of Shiraz University, Shiraz, Iran
[2]Department of Computer Science and Engineering, Faculty of Engineering of Shiraz University, Shiraz, Iran

Abstract: In this study Self-Organizing Map (SOM) neural network has been applied for clustering of high-dimensional geological and geophysical data of Iran resulting numerical tectonic zoning. Visualization of high-dimensional data in two-dimensional topology-preserving feature map (visualization of clusters) and also visualization of component planes (visualization of variables) are the other specific capabilities of SOM used in this study. The component planes constructed here by SOM are successful in determining the effective parameters in tectonic zoning. Although, there are some compatibilities between numerical maps constructed here and the conventional maps but SOM provides more detailed identification and reliable interpretation about different zones. Based on the especial properties of SOM, some similarities and dissimilarities between different zones, despite of their geographical positions, have been revealed that not been noticed in conventional map previously. According to the results of this study SOM is a powerful and suitable method in tectonic zoning especially for regions where their tectonic regionalization is not well known.

Key words: Tectonic zoning, self-organizing map, unsupervised clustering, neural networks, neotectonic homogenous region

INTRODUCTION

Iran has a long and rather complex tectonic evolution related to the multistage history of the Tethys domain (Meyer and Le Dortz, 2007), it represents the key locality on Earth to study upper crustal response to early process of continental collision processes due to the Late Miocene-Recent collision between Arabia, Eurasia and intervening cratonal rocks underlying Iran (Axen *et al*., 2001).

In order to understand the key role of Iran, tectonic zoning convert to different forms each bearing its own characteristics have been developed. Although, all these maps show some basic structures, there are differences among them mostly due to their qualitative definitions and assessments which are subjective (Zamani and Hashemi, 2004). The earliest one was proposed by Stahl (1911) that divided Iran geographically. The emergence of the concept of plate tectonic theory resulted in further geological interpretations of the country (Nowroozi, 1971). The most famous tectonic zoning belongs to Stocklin (1968) that recognized nine structural zones with different tectonic styles in Iran (Fig. 1). Aghanabati (1986), Berberian (1981), Berberian and King (1981), Boulin (1991), Choubert and Faure-Muret (1980), Davoudzadeh *et al*. (1986), Davoudzadeh and Weber-Diefenbach (1987), Eftekharnezhad (1980) and Nabavi (1976) subdivided Iran geologically into different tectono-sedimentary units based on orogenic history and structural style. Based on seismic data, Nowroozi (1976, 1979), Shoja-Taheri and Niazi (1981), Ambraseys and Melville (1982) and Karakaisis (1994) also subdivided Iran into different seismo-tectonic zones.

The conventional methods in tectonic zoning are deductive or top-down in their operation and are varied with the general objectives that influence the process of classifications, as dictated by prevailing philosophies. These methods are commonly characterized by two limitations. First, there is a large uncertainty involved in tectonic zoning based on non-quantitative and subjective analysis while the second is the difficulty to interpret accurately a large amount of geological data by naked eye. The human mind has a limited capacity that cannot grasp the characteristics of its complex surroundings in one operation.

So, despite the achievements in tectonic study, to avoid these deficiencies, it is necessary to find a quantitative method of tectonic zoning based on numerical criteria. Data mining refers to the application of a wide array of methods, ranging from relational learning to statistics and neural networks, to process and analyze data (Fayyad *et al*., 1996; Berthold and Hand, 1999; Hand *et al*., 2001). The aim is to extract knowledge from databases where the dimensionality, complexity, or amount of data is prohibitively large for manual analysis (Vesanto, 2002).

Corresponding Author: M. Nedaei, Department of Earth Sciences, Faculty of Sciences of Shiraz University, Shiraz, Iran

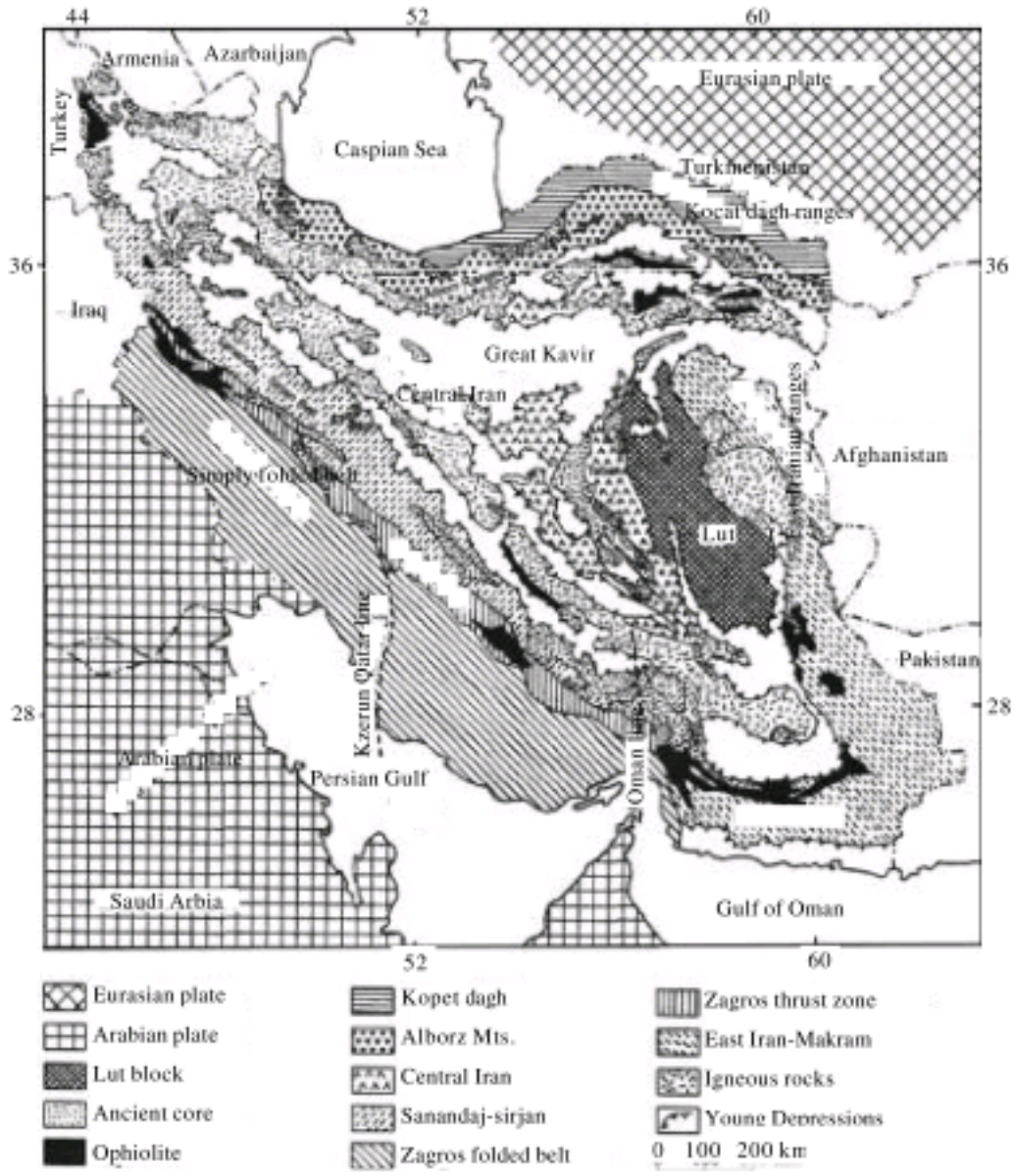

Fig. 1: Generalized tectonic map of Iran (adapted from Stocklin, 1968; Stocklin and Nabavi, 1973)

A technique that has been applied fruitfully for clustering and extracting interpretable patterns from large and complex data sets is the Artificial Neural Network (ANN). ANNs consist of a network of interconnected simple processing units or nodes that process information in parallel. Neural networks are specified by the characteristics of their neurons, network topology or architecture and the training or learning algorithms which define their purposes. On the basis of learning modes, ANNs are classified into two major types: supervised and unsupervised. In the supervised approach, classification of feature vectors is known and the final output of a neural network is compared to the desired output. In contrast, unsupervised learning is carried out without using any a priori classification of the samples. These networks monitor their performance internally.

This study focuses on the application of one common type of unsupervised ANN particularly adept at pattern recognition and clustering, the self-organizing map (SOM; Kohonen, 1984). SOM constitute a very well-known and widely used neural network model which employs unsupervised learning. Clustering and visualization are the main applications of SOM in data analysis. A particular strength of SOM is that it answers the needs of both tasks within a common framework. Because of these two important properties of SOM, the self-organizing map algorithm is a very valuable tool in the visualization and interpretation of large and multivariate data sets. An advantage of SOMs over other multivariate techniques is that the algorithm is robust in handling missing data, without a priori estimation.

The SOMs have been in a wide variety of areas including assessing beer quality, identification of breast cancer, analyzing insect courtship songs, predicting bankruptcies, speech and fingerprint recognition, performing searches on the WEB and in controlling autonomous robots (Kaski *et al*., 1998 for a database of these and other SOM papers arranged thematically). These have also been used extensively in the geographical sciences for synoptic climatology

(Hewitson and Crane, 1994; Hewitson and Crane, 2002). While SOM analysis is not a new subject, its application in tectonic regionalization has been utilized for the first time in this study.

The aim of this study is to present the SOM technique to researchers in the tectonic subject. It is not the intention of this study to give a detailed theoretical description of the SOM algorithm, which can be found in Kohonen (1984, 1997). Rather, it is meant to give a brief overview of the technique and thus demonstrate its utility by applying it to geological and geophysical data sets.

The goal of this study, an extension of Zamani and Hashemi (2004), hereafter referred to as I, is to improve and refine the new approach for multicharacteristic homogeneous tectonic regionalization using our new approach, SOM. To illustrate, this method has been applied for producing a general purpose multivariate numerical tectonic zoning maps of Iran.

TECTONIC SETTING

Iran belongs to a broad mobile belt of Tethys domain (Nowroozi, 1976) which is divided by several structurally significant active faults (Fig. 2). The main structural provinces of Iran are as follows:

On the southwest the Arabian Platform which is part of the Arabian basement shield is covered by young alluvial deposits. The platform is formed by a stable sequence of continental shelf deposits of late Precambrian to Tertiary age (Nowroozi, 1976). Structural deformations are limited to gentle undulations with axes following generally the south-north trend of Arabia (Stocklin, 1968).

The Zagros Fold-Thrust Belt lies on the northeastern margin of the Arabian platform and consists of a Phanerozoic succession with a stratigraphic thickness of up to 10 km that is folded into kilometer-scale simple anticlines and synclines (Stocklin, 1968). The present morphology of the Zagros active fold-thrust belt is the result of its structural evolution and depositional history: a platform phase during the Paleozoic; rifting in the Permian Triassic; passive continental margin (with sea-floor spreading to the northeast) in the Jurassic-Early Cretaceous; subduction to the northeast and ophiolite-radiolarite emplacement in the Late Cretaceous and collision-shortening during the Neogene (Berberian and King, 1981).

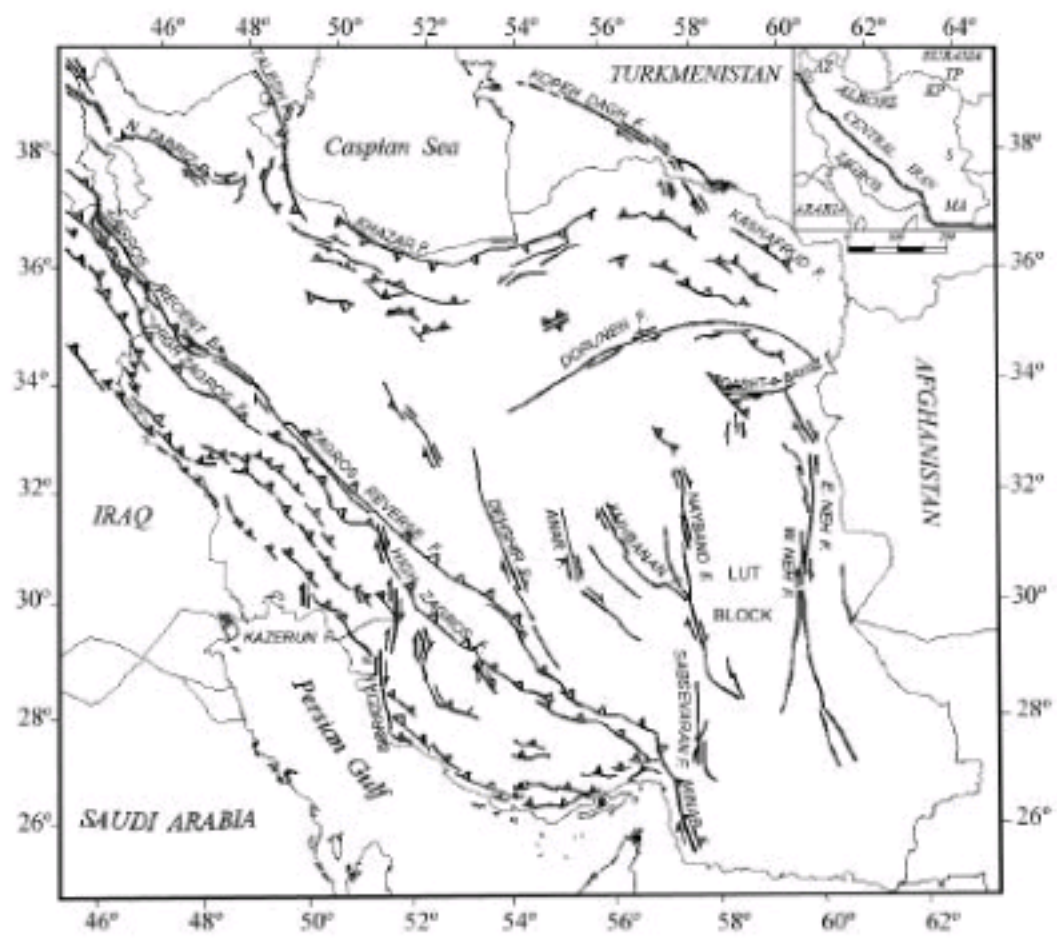

Fig. 2: Active faults of Iran and vicinity, modified from Berberian (1997). Reverse faults shown with teeth on hanging-wall side. Strike slip faults shown with arrows. Faults without teeth or arrows: sense of slip unknown. Inset: Map of Iran showing boundary with Arabian plate (line with teeth). AZ, Azarbaijan; KP, Kopeh-Dagh; MA, Makran deformation zone; S, Sistan suture

The crustal thickness (Dehghani and Makris, 1983 topography, intensity of deformation fold amplitude, reverse fault displacement, relative shearing along the Hormoz decollement detachment and age of the folded and faulted sedimentary rocks decrease from the High Zagros and the Zagros suture (the Main Zagros reverse fault) in the north and northeast toward the Zagros Foredeep in the south and southwest. Neogene and Quaternary folding in these units become younger from northeast to southwest demonstrating that the deformation front is migrating from the suture towards the foredeep.

The folded-thrust belt passes northeastward into a narrow zone of thrusting bounded on the northeast by the Main Zagros Thrust Line. The Main Zagros Reverse Fault indicates a fundamental change in sedimentary history, paleogeography, structure, morphology and seismicity. This important geological boundary called the Zagros suture, the Zagros Thrust Line or the Main Zagros Reverse Fault by various authors (Berberian, 1995), which marks the suture between the two colliding plates of the central Iranian active continental margin (to the northeast) and the Afro-Arabian passive continental margin (the Zagros fold-thrust belt to the southwest. In the NW Zagros a major NW-SE right-lateral strike-slip fault system roughly follows the Zagros Thrust Line called the Main Recent Fault.

The Sanandaj-Sirjan zone lies on the northeast of the Zagros Thrust Line. It has a length of 1500 km and the width of 200 km from northwest to southeast Iran and is characterized by metamorphic and complexly deformed rocks associated with abundant deformed and undeformed plutons in addition to widespread Mesozoic volcanic rocks. Volcanic of late Cretaceous-early Miocene age in the Sanandaj-Sirjan zone and central Iran represent Andeantype magmatism in southern Eurasia during Neo-Tethyan subduction. Volcanic and turbidite successions represent back-arc extension across central Iran, the Alborz and north of Neo-Tethyan subduction zone . In Central Iran this succession is commonly overlain by terrestrial clastics evaporaties and volcanics of Oligocene age.

The structural zone of Central Iran comprises a roughly triangular area limited by the Lut block on the east, the Alborz Mountains on the north and the Sanandaj-Sirjan Ranges on the southwest. Central Iran is separated from the Sanandaj-Sirjan Ranges by a continues zone of depressions including the Lake Rezayeh, Tuzlu Gol and Gavkhuni depressions and continuing into the Jaz Murian Depression of Iranian Baluchistan (Stocklin, 1968). A similar area of depression (the Kavir Depression) lies just south of the Alborz Mountain. Central Iran is a mosaic of various tectonic blocks once separated by minor ocean basins (Berberian and King, 1981) and the final closure of these basins may not have occurred until the mid-Tertiary (McCall, 1996). Pliocene time represents the final closure of any remaining ocean basins and the onset of true intra-continental shortening within Iran (Walker and Jackson, 2002). Jackson and McKenzie (1984, 1988) suggested mostly on the base of seismological observations that the Central Iranian Block can be regarded as rigid. The Lut block is an irregularly outlined, essentially north-south trending, rigid mass smoothly surrounded by the ranges of Central and East Iran. The Tabas is separated from the Lut by Shotori Range and the Nayband fault which has a north-south trend and may be related to older Precambrian fault zones on strike with the Oman trend (Stocklin, 1968). The NNW-SSE Shotori mountains form the highest topography (~2900 m) and are composed of heavily deformed Palaeozoic and Mesozoic rocks. The western boundary of the Tabas is the Kuhbanan fault.

The structurally east-west Makran Coastal Ranges of the south-eastern Iran is the continuation of the Zagros Mountains from the vicinity of Bandar Abbas to west Pakistan. It merges with the north-south trending East Iranian Ranges that lie east of the Lut Block. The deep sea basin south of the Makran coast is considered to be part of the remnant Tethys oceanic crust which has been suducting since Cretaceous times with a low angle under southeastern Iran and the Helmand Block (Ravaut *et al*., 1997). Subduction remains active and suturing has not yet occurred (Axen *et al*., 2001). The boundaries of the Makran wedge are quite complicated tectonic area. The eastern Ornah-Nal and Chaman fault zones and the western Minab-Zendan-Palami fault zone make transpressional strike-slip boundaries of the Makran. The western boundary forms a transition zone between the zagros continental collision and the Makran oceanic subduction (Stocklin, 1974; Falcon, 1976).

The Alborz Mountains are north of the Neo Tethyan sutured and wrap around the south Caspian Sea . The Alborz range consists mainly of late Precamberian to Eocene sedimentary and Paleogene andesitic volcanics and intrusive rocks. The Alborz Mountains are structurally and stratigraphically related to the Central Iran, but they were less strongly affected during the period of the initial Alpine orogeny. The Alborz Mountains started to rise in Eocene. Movements were renewed in Late Pliocene or Early Pleistocene marking their appearance as principally a volcanic range separating Central Iran from the Caspian basin to the north (Rieben, 1955).

The South Caspian Basin is a relatively aseismic block involved in the collision zone between Eurasia and

Arabia. This unusual thick basaltic lower crust (15-18 km) is overlaid by a thick sedimentary sequence (15-20 km).

East of the South Caspian Basin the Kopeh-Dagh is accommodating the deformation between the Turan to the north and the Lut-central Iran to the south. The NW flank of the Kopeh Dagh is assumed to be underlain by Hercynian basement of the Turan shield while the range itself contains thick Jurassic-Cretaceous marine sediments overlain by Eocene marls with some andesite volcaniclastic horizons.

The youngest folding in Iran occurred in Pliocene-Pleistocene time. Various morphotectonic features such as: the tilted Quaternary terraces, the mudvolcanoes and raised beaches, the fluctuations of the shorelines, the presence of Quaternary volcanoes, numerous active faults and recent earthquake activity are clear proof of continuing tectonic activity in Iran.

SELF-ORGANIZING MAPS

The architecture of the SOM is shown in Fig. 3. The SOM consists of one input layer and one output layer (Kohonen layer). An attractive characteristic of the SOM is the ability to map high-dimensional input space into low-dimensional space. The topological structure of the SOM can be one- or two-dimensional. Higher dimensions are acceptable but not common since their visualization is problematic. The SOM is trained using an unsupervised competitive learning algorithm which is a process of self-organization. The SOM algorithm can be described as follows.

Let M denote the dimension of input (data) space and an input pattern (vector) selected from input space be denoted by:

$$X = [x_1, x_2, ..., x_M]^T \quad (1)$$

The output layer includes the output neurons μ_j, j = 1, 2..., N, where N is the total number of output neurons in the network which are typically organized in a planar

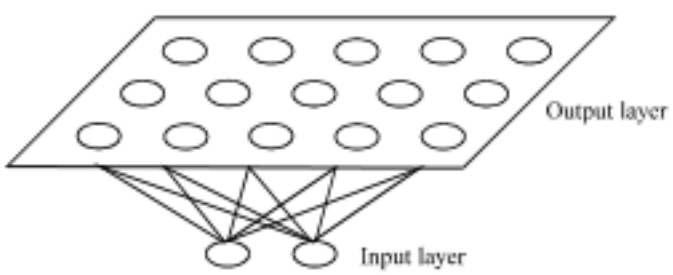

Fig. 3: Architecture of the self-organizing map. Each neuron in this SOM structure represents a geological cluster

(2D) lattice. The weight vector of each neuron which is known as prototype vector, too, has the same dimension as the input pattern. The weight vector of neuron j can be written as:

$$W_j = [w_{j1}, w_{j2}, ..., w_{jM}]^T, \ j = 1, 2, ..., N \quad (2)$$

The training process begins with all weights initialized to small random numbers. The SOM algorithm computes a similarity (distance) measure between the input vector X and the weight vector W_j of each neuron μ_j. The Euclidean distance d_j between the weight vector W_j and input vector X is frequently used as the similarity measure

$$d_j = \|X - W_j\| = \sqrt{\sum_{i=1}^{M} (x_i - w_{ji})^2} \quad (3)$$

The output neuron with the weight vector that is the smallest distance from the input vector is the winner. The Best Matching Unit (BMU) or the winning neuron, denoted here by μ^*_j, is determined by applying the condition:

$$u_j^* = \arg\min_j \{\|X - W_j(t)\|\} \quad (4)$$

The weights of this winning neuron are adjusted in the direction of the input vector. Not only the winning neuron but also the neurons in the topological neighborhood of the winning neuron are affected by the competition. The influence of competition decays symmetrically from the winning neuron location. The winning neuron is the center of the topological neighborhood. A typical choice of topological neighborhood function is Gaussian function:

$$h_i = \exp\left(-\frac{\|u_j - u_j^*\|^2}{2\sigma^2}\right) \quad (5)$$

where h_i is the topological neighborhood, σ is the effective width of the topological neighborhood.

The change to the weight vector W_j can be obtained as:

$$\Delta W_j = \eta h_i (X - W_j) \quad (6)$$

where, η is the learning-rate parameter of the algorithm. Hence, the updating weight vector W_j (t+1) at time (t+1) is defined by (Kohonen, 1982)

$$W_j(t+1) = W_j(t) + \eta(t) h_i(t) (X - W_j(t)) \quad (7)$$

where, η (t) and h_i (t) are the learning-rate parameter and the topological neighborhood at time t, respectively.

Equation 7 is applied to all the neurons in the lattice that lie inside the topological neighborhood of winning neuron. The learning-rate parameter η (t) is time varying as indicated in Eq. 7. In particular, η (t) starts at an initial value and then decreases gradually with increasing time. Upon repeated presentations of the training data, the weight vectors tend to move toward the input pattern due to the neighborhood updating. The algorithm therefore leads to a topological ordering of the output layer (which is known as the feature map) in the sense that neurons that are adjacent in the lattice will tend to have similar synaptic weight vectors. The winning neuron shows the topological location of the input pattern. The neighborhood of the winning neuron shows the statistical distribution of the input pattern. Thus the feature map is a topology-preserving map (Kohonen, 1995). The output of the SOM shows the neurons that are winning each pattern. In addition, there is also a measure which determines how well each input instance is represented by Self Organized Map (SOM). The quantization error measures the resolution of the SOM and is calculated as the average total Euclidian distance between an input vector and the reference vector of its best matching unit (Kohonen, 1995). Thus a large error for a particular input sample means that it is not well represented by the pattern it was mapped to.

The SOM has also vector projection properties that preserve the order of distances between all originally high-dimensional objects in low-dimensional coordinates. As mentioned above the SOM orders -or projects- prototype vectors (weight vectors) on a predefined map grid such that local neighborhood sets in the projection are preserved: if two data samples are close to each other in the visualization, they are more likely to be close in the original high-dimensional space as well (Venna and Kaski, 2001).

In the visualizations, the SOM acts in two roles: cluster visualization and variable visualization. In visualization techniques the prototype vectors or in brief prototypes of the SOM are regarded as a representative sample of the data.

The most widely used methods for visualizing the cluster structure of the SOM are distance matrix techniques (Ultsch and Siemon, 1990), especially the unified distance matrix (U-matrix). In this technique, the Euclidean distances between each unit (neuron) i and the units in its neighborhood are calculated. A unit with a large U-matrix value is dissimilar to the neighboring units; on the other hand, a unit with a small U-matrix value is similar to the neighboring units. Therefore, cluster borders can be identified as mountains of high distances separating clusters as valleys of low distances. This visualization enables us to recognize the degree of similarity among adjacent units in the two-dimensional map.

To visualize variables using the SOM, a technique called component planes is used. For each visualized variable, or vector component, one SOM grid is visualized such that the colors of the map units change according to the visualized values. Relationships between variables can be seen as similar patterns in identical places on the component planes: whenever the values of one variable change, the other variable changes, too (Vesanto and Ahola, 1999).

DATA SOURCE

In this study, data mining based on SOM contains several phases: (1) data collection, (2) preprocessing, (3) normalization, (4) SOM training, (5) clustering and visualization and (6) interpretation of clusters.

In the first stage for the purpose of data collection, Iran is divided into 175 quadrangles, each covering a degree of latitude and longitude (Zamani and Hashemi, 2000, 2004). The quadrangles from west to east are numbered beginning from 1 for the quadrangle between 44 and 45°E meridians and increasing to 175 for the quadrangle between 61 and 62°E meridians. These quadrangles make input samples (observations) and all possible measures of tectonic characteristics in the region of 1° areas are considered as features (variables) for each input sample. Data collection consists gathering these features for each quadrangle from available maps or catalogs.

As we know tectonics is predominantly the study of the history of motion and deformation on a regional to global scale that preserved in the rocks. Geophysical data are important to tectonics. Seismic, magnetic and gravity data provides information on the geometry of large-scale structure at depth, which adds the critical third spatial dimension to our observations. Tectonics also depends on other branches of geology. Petrology and geochemistry provide data on the temperatures, pressures and age of deformation and metamorphism which permit accurate interpretation of deformation and its tectonic significance. So, in our study all of the available geophysical and geological data are considered as tectonic features.

The quality and quantity of data sets was increased respect to paper I. The list was made as complete as possible. The eventual controlling criterion, however, was whether the information on each variable could be

extracted from the available data. From the whole 49 variables, 14 are concerned with geological, 6 with seismicity and 29 with other geophysical characteristics of the region. Table 1 shows these geophysical and geological variables as the dimension of SOM input vectors.

Digital geological maps gained from GSI were correlated with geological Oil Co. maps of Iran then using ArcView software, geological data were obtained. Seismicity data have been achieved from earthquakes that occurred between the years 1900 to 2007 (Engdahl *et al*., 2006; Gutenberg and Richter, 1954). Also a and b value were obtained by z-map software. Then the seismicity data were smoothed for each quadrangle by the weights of Shoja-Taheri and Niazi (1981). This is done because of uncertainty location of epicenter points that being very crucial for marginal data. Other geophysical data were taken from Dehghani and Makris (1983), magnetic intensity map and digital data from Geological Survey of Iran (GSI).

In preprocessing phase of our investigation, all variables were given equal weight. Although it is possible to weight variables, various investigators question the validity of such a procedure (Gordon, 1999), because weights can only be based on intuitive judgments of what is important. So, as there is no reliable information about the relevance of different variables in tectonic zoning, equal weighting would seem appropriate.

It is clear from Table 1 that geological data, representing outcropping geology, compose only 30% of the whole. The rest of the data belongs to geophysical data that bring us valuable information about physics and dynamics of the crust. In fact, correct interpretation of tectonic history of any region needs surficial and subsurficial information.

Table 1: Geophysical and geological variables used by SOM for regional tectonic zoning of Iran

No. of variables	Measured variables in 1° quadrangle
Geophysical variables	
1	Minimum magnetic intensity (gamma), MIMGI
2	Maximum magnetic intensity (gamma), MXMGI
3	Range of magnetic intensity (gamma), RAMGI
4	Average magnetic intensity (gamma), AVMGI
5	Minimum gravity anomaly (mgal), MIGRV
6	Maximum gravity anomaly (mgal), MXGRV
7	Range of gravity anomaly (mgal), RAGRV
8	Average gravity anomaly (mgal), AVGRV
9	Minimum free air anomaly (mgal), MIFRA
10	Maximum free air anomaly (mgal), MXFRA
11	Range of free air anomaly (mgal), RAFRA
12	Average free air anomaly (mgal), AVFRA
13	Minimum Bouguer anomaly (mgal), MIBUG
14	Maximum Bouguer anomaly (mgal), MXBUG
15	Range of Bouguer anomaly (mgal), RABUG
16	Average Bouguer anomaly (mgal), AVBUG
17	Minimum isostatic anomaly (mgal), MIISO
18	Maximum isostatic anomaly (mgal), MXISO
19	Range of isostatic anomaly (mgal), RAISO
20	Average isostatic anomaly (mgal), AVISO
21	Average Moho depth (km), AVMOD
22	Minimum regional anomaly (mgal), MIREG
23	Maximum regional anomaly (mgal), MXREG
24	Range of regional anomaly (mgal), RAREG
25	Average regional anomaly (mgal), AVREG
26	Minimum residual anomaly (mgal), MIRES
27	Maximum residual anomaly (mgal), MXRES
28	Range of residual anomaly (mgal), RARES
29	Average residual anomaly (mgal), AVRES
Geological variables	
30	Minimum elevation (m), MIELV
31	Maximum elevation (m), MXELV
32	Range of elevation (m), RAELV
33	Average elevation (m), AVELV
34	Relative area of Cenozoic rocks (%), RACER
35	Relative area of Mesozoic rocks (%), RAMER
36	Relative area of Paleozoic rocks (%), RAPAR
37	Relative area of Proterozoic rocks (%), RAPTR
38	Relative area of Igneous rocks (%), RAIGR
39	Relative area of metamorphic rocks (%), RAMER
40	Relative area of ophiolitic rocks (%), RAOPR
41	Relative area of sedimentary rocks (%), RASER
42	Relative area of unconsolidated rocks (%), RAUNR
43	Fault length density (k m^{-1}), FLTLD
Seismicity variables	
44	Number of earthquakes smaller than m_c, NESMC
45	Number of earthquakes greater than m_c, NEGMC
46	Maximum earthquake magnitude (m_b), MXEMG
47	Maximum seismic energy released (j), MXSER
48	b-value in the Gutenberg-Richter's formula, BVGRF
49	a-value in the Gutenberg-Richter's formula, AVGRF

DATA ANALYSIS AND RESULTS

The basic data are set out in a m*n matrix consist of n variables made on m quadrangular sites. Each row represents one observation and each column represents one variable or attribute. In this study m comprises of 175 quadrangular sites as described before and n consists of 49 attributes used as possible measures of tectonic characteristics of the region under investigation (Table 1).

As most distance measures between clusters are based on distances between individual data vectors so they are sensitive to the scales of the variables. Therefore data vectors must be normalize. For this purpose the most common standardization procedure, Z-score method, is applied. This method treats all variables independently and transforms each by subtracting the mean and dividing by the standard deviation of each variable. In normalization phase, all 175 input vectors were normalized among each variable by z-score method.

In SOM construction, we preferred a hexagonal lattice as the hexagonal ordering provides more neighbors to each unit. In the SOM training phase, freely available Matlab Package SOM Toolbox was used (http://www.cis.hut.fi/projects/somtoolbox/).

There is no theoretical principle for determining the optimum size of the output layer and hence the output layer is kept large enough to ensure that the best clustering is achieved. To select the best SOM configuration, resulting the best clustering, some kind of validity index can be used. In our investigation, we used the Davies-Bouldin index (Davies and Bouldin, 1979), which uses S_c for within-cluster distance as:

$$S_c = \frac{\sum_i \|x_i - c_k\|}{N_k} \quad (8)$$

where, C is the number of clusters, Q_i is a set of clusters, i = 1,2,... C; N_k is the number of samples in cluster Q_k and

$$c_k = \frac{1}{N_k} \sum_{x_i \in Q_k} x_i$$

is the center of cluster C_k. This index also uses $d_{ce} = |c_k - c_l|$ for between clusters distance. According to Davies-Bouldin validity index (DBI), the best clustering minimizes

$$\frac{1}{C} \sum_{k=1}^{C} \max_{l \neq k} \left\{ \frac{S_c(Q_k) + S_c(Q_l)}{d_{ce}(Q_k, Q_l)} \right\} \quad (9)$$

The index gets low values for clusters which are compact and far from the other clusters.

Different map topology (different map units) was trained to evaluate the best one among them. We examined 5-230 number of map units in order to distinguish the optimum size of output layer using DBI. The maps were trained using the batch training algorithm in two phases: a rough training with large initial neighborhood width and 0.5 learning rate and a fine-tuning phase with small initial neighborhood width and 0.05 learning rate. The neighborhood width decreased linearly to 1; the neighborhood function was Gaussian. The training lengths of the two phases were 11 and 44 epochs. The learning rate decreased linearly to zero during the training. After the training phase, the SOM consists of a number of patterns characteristic of the data, with similar patterns nearby and dissimilar patterns further apart.

Among different map units examined (up to 230 units), the best map configuration according to DBI was [16 12], 192 units, that created 19 clusters (Fig. 4). Next, to identify the relationship between clusters and also variables the trained SOM with 192 units was visualized by U-matrix, feature map and component planes representations. U-matrix visualization indicates the number of valleys (clusters) enclosed by mountain ridges (cluster boundaries) (Fig. 5a). Feature map represents the

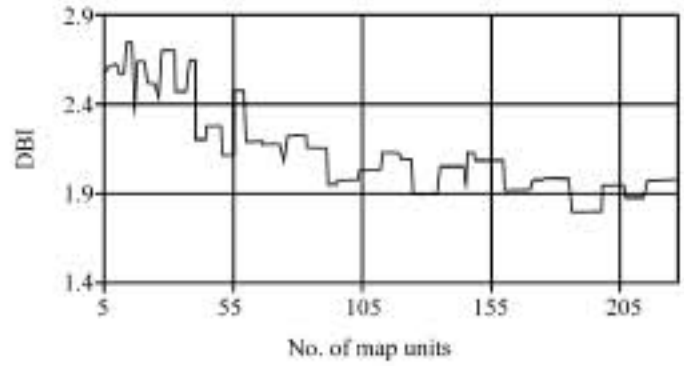

Fig. 4: Davies-Bouldin index as function of the number of map units. As it is shown minimum DBI is belonged to 192 units that create 19 clusters

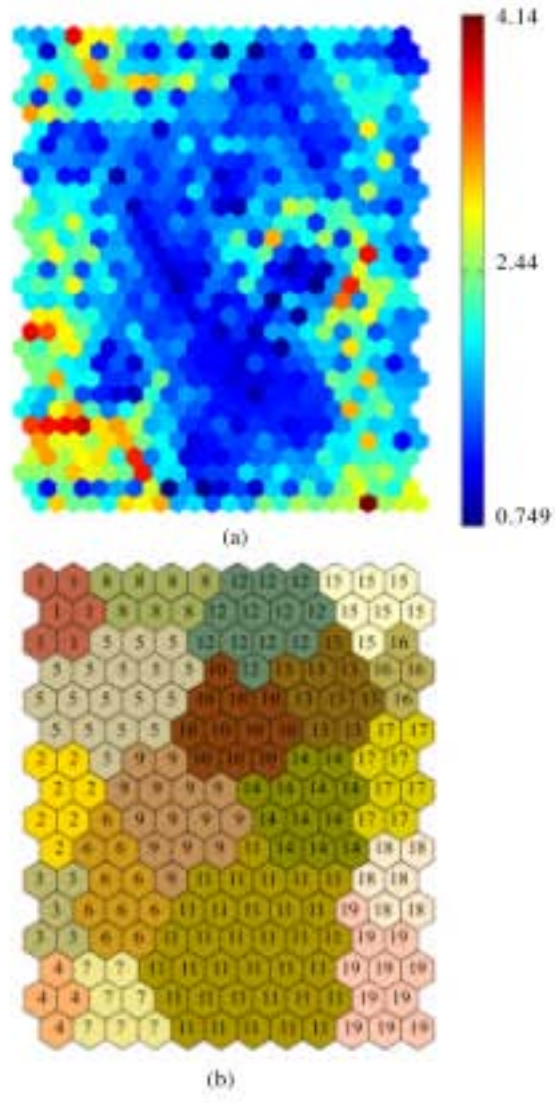

Fig. 5: Visualizations of (a) U-matrix that shows distance between units and (b) SOM feature map that represents clusters and their positions and neighbors on the map

position of clusters and their neighbors (Fig. 5b). As each cluster is distinct in feature map, other SOM visualization can be well interpreted by it.

We also constructed the component planes of our map (Fig. 6). Each component plane shows the value of

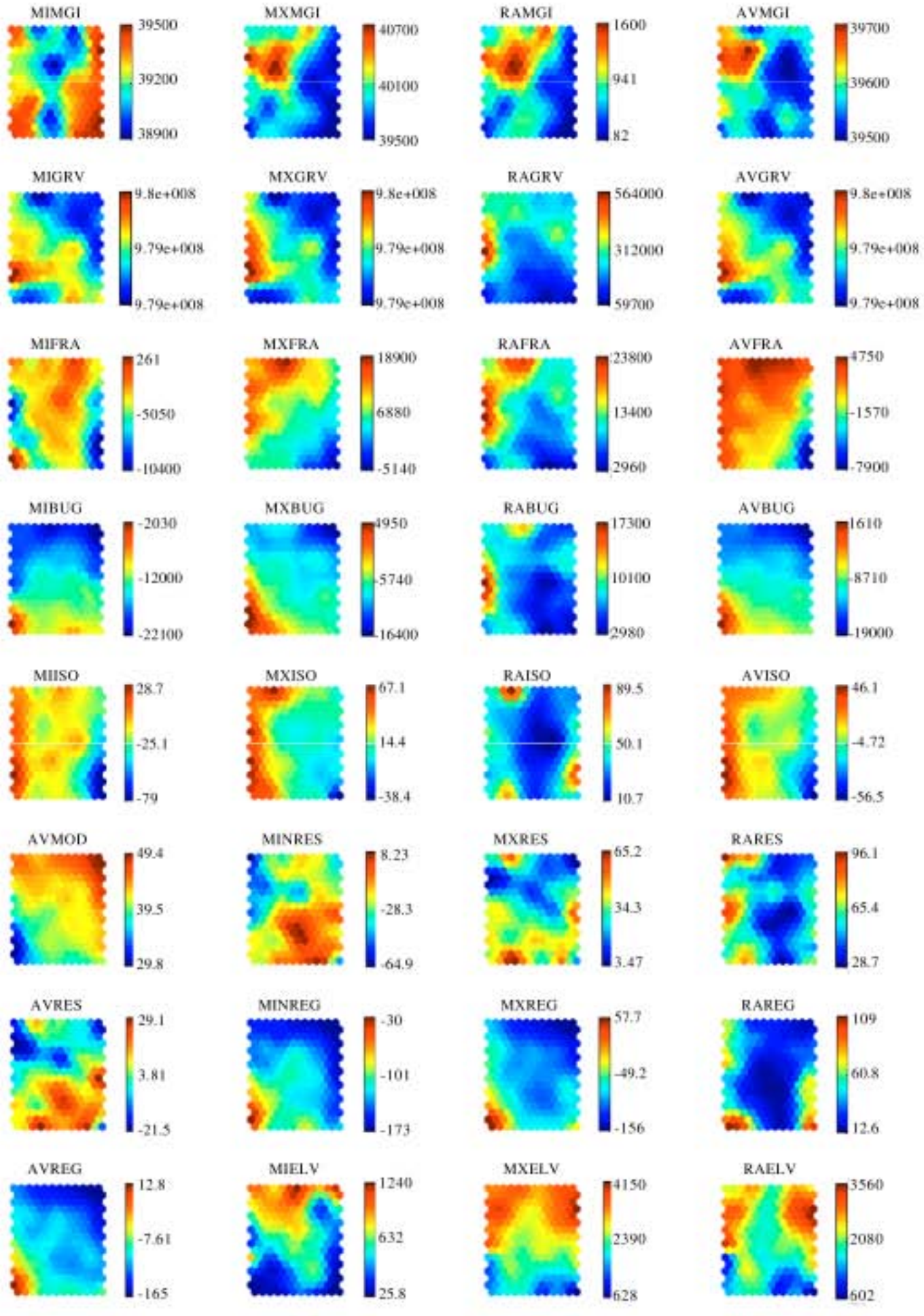

Fig. 6: Continued

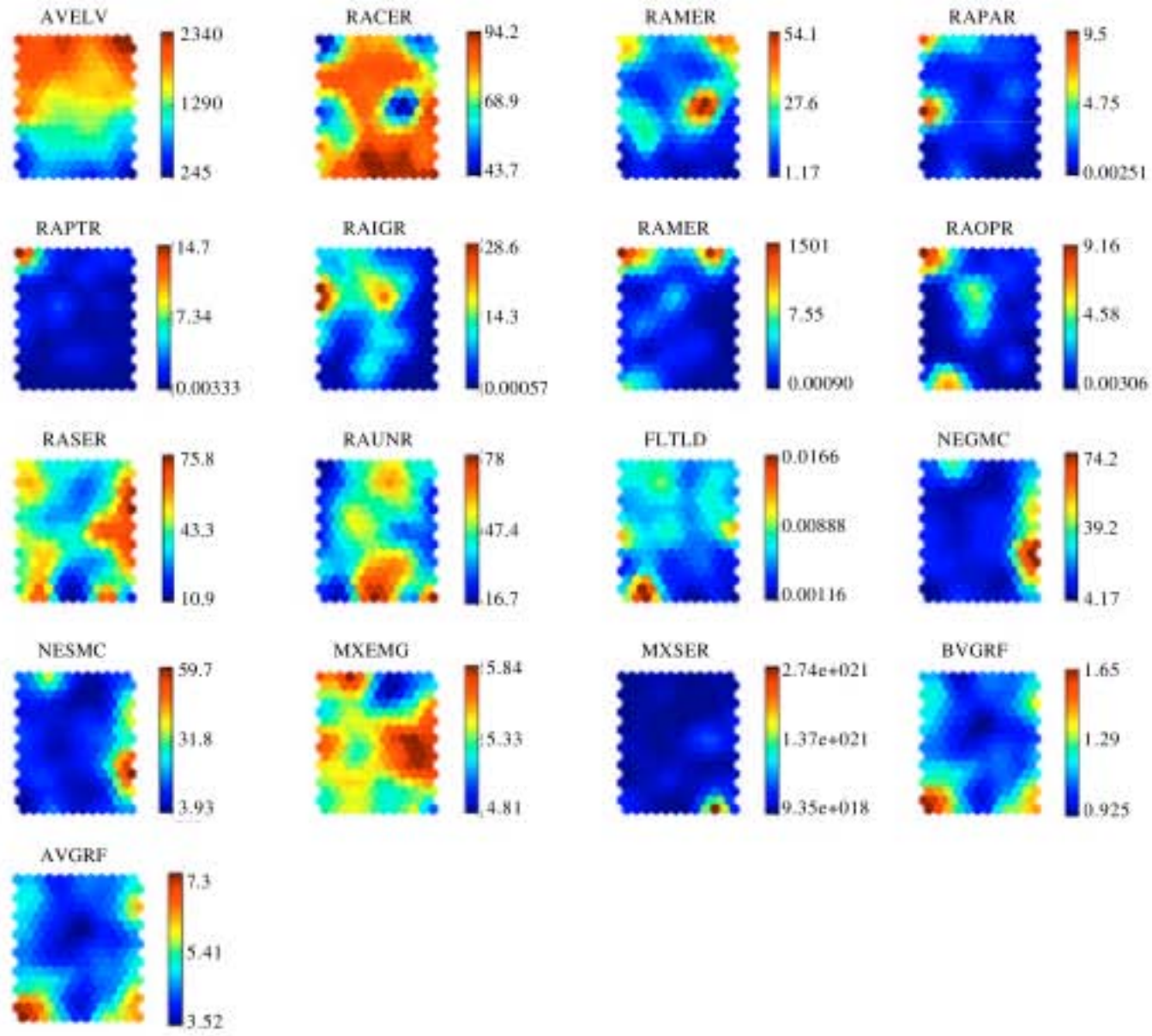

Fig. 6: Component planes of earlier SOM that represent the value of each variable in each map unit

one variable in each map unit. As identical unit has fixed place and equal size in different component planes, they can be easily compared and the relationship between variables and their distribution within the clusters can be checked. Therefore the correlation between variables is seen as similar patterns in identical places on component planes. As it is shown in Fig. 6 some variables are dependant: 2 and 3, 5, 6 and 8, 13, 14 and 16, 18 and 20, 26, 27 and 29, 44 and 45, 48 and 49. The variables 2, 5, 6, 13, 14, 18, 26, 27, 44 and 49 are redundant and may misguide clustering results. Except from these variables other planes appear to be suitable for clustering discrimination. Based on this assumption, redundant variables were deleted. Then the new SOM was trained for new combination of remained variables. Early- and end-SOMs have 3.676 and 3.374 quantization error, respectively. It means end-SOM well represents the pattern it was mapped to and also demonstrates that deleting the redundant variables causes better performance (and consequently better clustering) of SOM than with total variables. Final clustering has a better detection of tectonic zones than it is done with total variables.

DISCUSSION

After removing redundant variables, the result of the clustering roughly indicates 19 main different clusters (Fig. 7). Geophysical and geological variables of each clusters or tectonic zones is presented in Table 2. The zones created by SOM were located on the map of Iran and are as follows (Fig. 8).

Zone 1 is magmatic zone and has a wide variety of elevation. This structural zone extends parallel to the Zagros thrust. In this zone elevation and percentage of igneous rocks are the important features. The residual anomaly and the average of Moho depth in this zone indicate an increase of thickness crust may be due to the

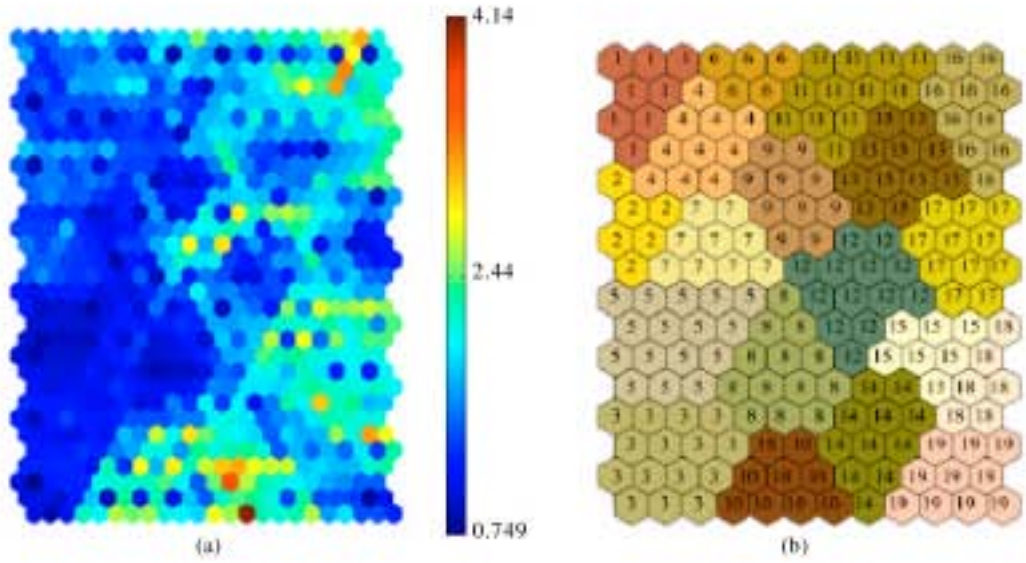

Fig. 7: (a) U-matrix and (b) SOM feature map visualizations show the result of final SOM (after removing redundant variables)

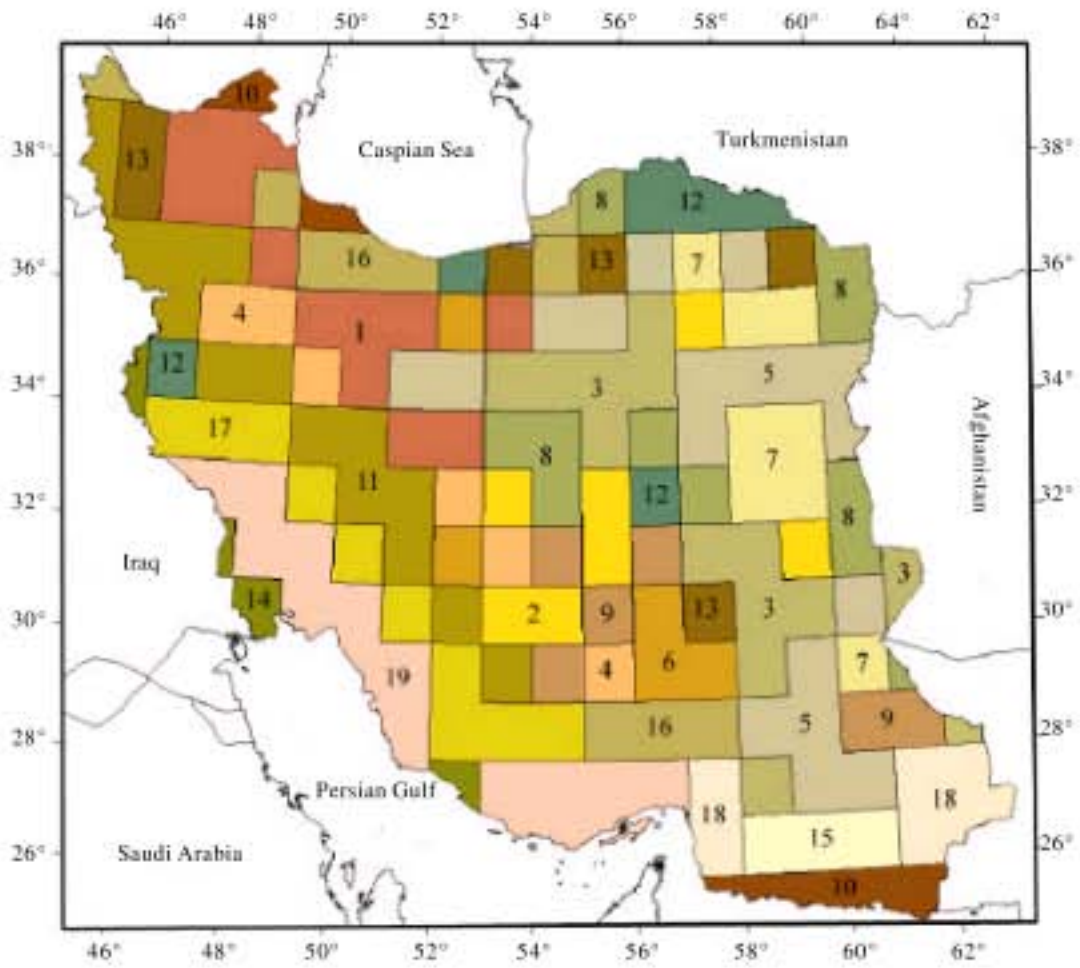

Fig. 8: Numerical tectonic zoning in Iran using SOM, colors and numbers of the clusters are the same as Fig. 6b

magmatic activity and thrust faulting. It is nearly corresponding to Rezaiyeh Province of Nowroozi (1976).

Zone 2 indicates the metamorphic rocks of Protrozoic that mark the boundaries of the internal Iranian microcontinental block along its major faults. It is not separated in conventional map. Magnetic intensity is another important feature of this zone. In this zone variation range of magnetic intensity is high.

Zone 3 consists of the Great Kavir, Lut and Zabol blocks. It is relatively in isostatic equilibrium. These three regions aren't considered as a unique zone anywhere.

Zone 4 separates Central Iran from the Sanandaj-Sirjan zone including Tuzlu Gol and Gavkhuni depressions

Table 2: Geophysical and geological variables of 19 automated tectonic zones presented in Fig. 9. Units and symbols are the same as Table 1

No.	MIMGI	RAMGI	AVMGI	RAGRV	AVGRV	MIFRA	MXFRA	RAFRA	AVFRA	RABUG	AVBUG	MIISO	RAISO	AVISO	AVMOD	MIREG	MXREG	RAREG	AVREG	RARES
1	39246.77	1366.77	39692.15	369353.08	979408879.52	-3740.77	15113.85	18854.62	4143.15	9591.54	-12723.17	3.77	32.77	20.34	41.86	-38.46	16.62	55.08	-10.57	55.92
2	38780.00	1978.86	39535.86	213718.57	979067348.16	-2125.71	8368.57	9711.43	2402.21	6161.43	-13795.28	-16.86	22.00	0.69	44.26	-22.43	15.86	38.29	-2.88	16.57
3	39241.50	654.20	39525.78	121897.06	979329086.18	-3554.12	2847.06	6401.18	-419.22	5055.88	-8027.17	-18.00	24.18	-2.05	39.80	0.71	42.24	41.53	21.45	21.18
4	39262.17	736.17	39573.17	167718.33	979074809.58	-1730.00	13220.00	14950.00	4774.02	9001.67	-15352.20	2.83	31.67	18.69	45.76	-17.17	25.50	41.00	6.40	26.33
5	39079.11	933.50	39533.69	159058.89	979281352.74	-3692.22	6340.56	9699.44	-7.25	5951.67	-9882.58	-20.94	27.67	-7.02	41.91	-16.39	29.06	45.28	6.34	21.78
6	39051.20	893.40	39437.20	327440.00	978896618.12	-2048.00	21134.00	23182.00	4999.42	12372.00	-16164.24	-16.40	50.60	11.23	44.04	-46.00	18.80	64.80	-13.15	26.20
7	39144.63	975.25	39535.25	210337.50	979223349.37	-1995.00	7876.25	9871.25	2471.10	7478.75	-12957.91	-17.00	17.38	-8.50	43.43	-45.88	10.50	56.38	-18.05	18.88
8	39305.09	577.64	39511.37	217020.00	979304383.90	-3000.00	8371.82	11371.82	2112.34	6591.82	-9524.14	-11.64	24.55	2.63	39.07	-0.82	41.45	42.27	20.33	16.36
9	39120.17	710.17	39450.67	284028.33	978875114.29	-1510.00	11661.67	13171.67	3380.38	6471.67	-14185.39	-17.00	28.33	1.43	43.49	-24.83	22.33	47.17	-0.55	24.50
10	39406.14	376.85	39541.93	142431.25	979500818.05	-2810.00	7935.00	10745.00	2806.02	9708.75	587.08	26.40	35.33	44.96	29.58	-15.95	44.38	60.33	14.54	77.20
11	39391.20	599.27	39595.80	248054.67	979151603.46	-2570.00	9584.00	12154.00	3601.64	6570.00	-16686.97	-9.27	35.73	9.60	47.43	-40.73	17.87	58.60	-11.19	41.20
12	39390.63	242.38	39497.71	188713.75	979525490.75	-3218.75	4212.50	7431.25	610.24	3535.00	-10153.13	3.25	12.13	8.90	41.61	-21.13	11.13	32.25	-5.62	25.63
13	39267.33	814.67	39566.58	371413.33	979481366.92	-4266.67	10991.67	15258.33	2001.35	9691.67	-10944.31	-3.17	33.00	14.67	41.14	-37.17	40.33	77.50	2.91	36.00
14	39521.02	72.76	39549.70	56683.33	979361269.25	-7521.67	-3381.67	4140.00	-4897.73	3511.67	-7009.15	-40.00	23.17	-26.00	39.58	-32.50	17.00	49.50	-7.57	55.00
15	39449.00	788.00	39636.83	221920.00	978889848.56	-2216.67	6356.67	8446.67	2742.37	9880.00	-4544.70	-14.00	54.00	11.16	37.39	-36.67	28.00	64.67	-3.68	91.67
16	39194.67	764.67	39560.39	491418.89	979331991.99	-10066.67	15058.89	25125.56	2480.83	15302.22	-11025.36	-8.44	79.67	30.72	39.18	-40.56	55.78	96.33	7.24	47.67
17	39483.70	93.90	39528.95	265640.00	979051543.09	-6558.00	5906.00	12464.00	-1264.47	8572.00	-13591.21	-31.80	43.40	-9.98	47.29	-24.10	30.00	54.10	2.07	35.10
18	39345.33	522.67	39495.83	189306.67	978853560.91	-5560.00	4596.67	10156.67	-648.70	7826.67	-9332.55	-36.17	63.33	-3.91	37.92	9.17	87.00	77.83	48.85	88.50
19	39446.85	114.08	39498.42	166372.62	979155154.62	-9965.38	-520.77	9479.23	-6436.73	5136.15	-9624.51	-71.15	68.62	-37.82	43.02	-14.15	39.62	53.77	14.31	74.46

No.	AVRES	MIELV	MXELV	RAELV	AVELV	RACER	RAMER	RAPAR	RAPTR	RAIGR	RAMER	RAOPR	RASER	RAUNR	FLTLD	NEGMC	MXEMG	MXSER	BVGRF
1	-103.50	965.38	3100.00	2134.62	1956.08	88.07	8.86	0.92	0.51	22.15	0.52	0.01	37.48	38.19	0.01	7.43	5.18	7.12932E+19	1.11
2	-131.22	828.57	2814.29	1985.71	1538.44	76.89	16.39	2.30	4.41	8.41	5.72	1.55	25.40	58.90	0.00	4.48	5.02	1.21834E+19	1.03
3	-103.14	458.82	1558.82	1100.00	824.79	93.07	4.04	0.40	0.46	4.96	0.51	0.81	22.04	69.65	0.00	6.76	5.25	8.2246E+19	1.02
4	-151.90	1133.33	3166.67	2033.33	2060.10	84.67	13.22	1.12	0.98	6.74	5.36	0.50	30.84	56.57	0.00	6.94	4.95	5.23541E+19	1.08
5	-106.95	455.56	2644.44	2188.89	1303.13	90.40	6.71	1.35	0.52	10.97	1.81	0.79	24.75	60.67	0.01	9.91	5.61	1.3181E+20	1.12
6	-129.22	1170.00	4180.00	3010.00	2411.01	80.04	15.29	3.99	0.68	12.87	0.07	1.22	47.49	38.34	0.01	15.86	5.59	1.42278E+20	0.99
7	-107.29	881.25	2750.00	1868.75	1714.26	87.32	11.46	0.77	0.46	18.28	1.64	6.62	29.23	44.24	0.00	11.83	5.64	6.87325E+19	1.00
8	-102.07	545.45	2509.09	1963.64	1300.31	72.11	24.56	2.18	1.15	5.42	1.60	1.14	43.65	48.19	0.01	5.69	5.11	1.41059E+19	1.02
9	-135.21	116.67	3516.67	3400.00	1763.79	80.84	15.73	1.99	0.82	7.33	3.10	1.35	38.29	49.30	0.01	5.95	5.14	3.97934E+19	1.02
10	-6.87	75.00	1337.50	1262.50	458.95	77.24	3.41	0.07	0.40	1.34	4.51	0.00	40.76	34.51	0.00	7.13	5.30	2.33873E+20	1.43
11	-146.02	1050.00	3520.00	2470.00	2282.68	48.76	40.01	3.00	7.68	5.08	12.68	4.31	47.87	29.51	0.01	13.29	5.28	5.60214E+19	1.16
12	-99.47	468.75	2875.00	2406.25	1529.58	37.34	57.70	0.89	0.06	2.36	0.20	1.68	68.49	23.26	0.01	15.18	5.81	5.21818E+20	1.11
13	-107.69	458.33	3133.33	2675.00	1748.63	59.67	22.71	5.48	1.34	3.01	3.33	0.06	44.22	38.58	0.01	14.93	5.70	1.5979E+20	1.07
14	-65.30	41.67	1316.67	1275.00	439.81	83.70	9.59	0.00	0.00	0.00	0.00	0.00	50.01	43.28	0.00	15.96	5.15	5.67249E+17	1.39
15	-39.88	133.33	2000.00	1866.67	882.45	85.51	13.25	1.24	0.00	0.06	5.29	10.26	68.57	15.83	0.02	5.19	5.26	1.74914E+20	1.68
16	-101.24	316.67	3577.78	3261.11	1876.75	63.47	20.92	7.91	2.98	18.42	6.20	2.57	40.78	27.32	0.01	27.61	5.80	8.69945E+19	1.05
17	-143.73	387.53	3673.00	3285.47	1698.88	75.11	23.64	0.86	0.22	0.30	0.25	0.37	75.39	23.52	0.00	38.11	5.68	1.42993E+20	1.26
18	-102.62	108.33	2183.33	2075.00	1095.61	91.91	4.99	1.49	0.23	0.56	2.80	4.36	69.47	21.43	0.02	14.85	5.70	1.88952E+21	1.16
19	-113.74	55.77	2096.15	2040.38	739.98	86.45	4.82	0.30	0.30	0.00	0.00	0.00	52.65	39.23	0.00	50.32	5.58	1.51187E+20	1.29

and continued into Jaz-Murian depression. Minimum of elevation and maximum free air anomaly play a substantial role to separate this zone from the others.

Zone 5 contains Jaz-Murian, Kashmar and Jajarm-Damghan-Qom depressions. Jaz-Murian depression is approximately correlated with Jaz Murian Province of Nowroozi (1976) and Jaz Murian depression of Stocklin (1968) but Northern parts of this zone (Kashmar and Jajarm-Damghan-Qom depression) have not been appeared in any conventional map. In this zone magnetic intensity and percentage of igneous rocks are considerable.

Zone 6 demonstrates igneous rocks majority of Paleozoic. It is nearly a seismic zone in which the range of maximum earthquake magnitude is high. Free air anomaly and magnetic intensity are also important features in this zone. By considering the relatively low distance between two neighboring zones 1 and 6 in Fig.7, it seems to be the continuation of zone 1 to the southeast, but it is separated from zone 1 because of its higher free air anomaly. This zone isn't considered as an individual zone in conventional map.

Zone 7 is Ferdows and Torbat blocks. This zone is differentiated from around by relatively high percent area of igneous and ophiolitic rocks.

Zone 8 includes Yazd, Nayband and Kalmard blocks and also south of Sarakhs. Only in our results, these blocks are separated from Central Iran. This zone contains highly faulted Mesozoic rocks.

Zone 9 represents Bazman and Taftan volcano and some related magmatic area in Central Iran. This zone has not been cleared in any conventional map and is separated from zone 1; it may be due to the activity of the southern part of Urumiyeh-Dokhtar magmatic arc that is associated with ongoing subduction of Indean ocean crust (Alavi, 1994). It exclusively consists of Mesozoic and Cenozoic rocks.

Zone 10 is some regions in north and south in which residual and regional anomaly play important role. Moho depth is also at lowest value in this zone.

Zone 11 consists of metamorphic and ophiolithic rocks of Protrozoic and Paleozoic from Sanandaj to Neyriz and approximately is similar to Sanandaj-Sirjan zone of Stocklin (1968). This zone has structurally dominant northwest-southeast trend. The residual anomaly of this zone indicates an increase of thickness crust may be due to the magmatic activity and thrust faulting.

Zone 12 is composed of Kopeh-Dagh, Kermanshah and Tabas Block. Free air anomaly is minimum in this zone. This zone is relatively seismic and faulted. Majority of this zone is composed of Mesozoic rocks.

Zone 13 includes some similar regions such as Gorgan schists and ophiolites in Mashhad. Eftekharnezhad and Behroozi (1991) depicted that Gorgan schists is comparable with accretionary prism of the remnant old Tethys in Mashhad and metamorphosed by Late Cimmerian. Kerman is also located in this zone. This zone does not appear in conventional tectonic zoning. Fault length density is high in this zone. It contains Mesozoic rocks that almost metamorphosed.

Zone 14 is Arabian platform. It is equivalent to the Plain of Shatt-al-Arab of Stocklin (1968) and Arvand Shatt-al-Arab province of Nowroozi (1976). It exclusively consists of sedimentary rocks and has minimum residual anomaly.

Zone 15 illustrates Makran ranges that are mainly east to west. It has maximum fault density and is a relatively high seismic zone. The other important feature in this zone is b value that insists on the active subduction of Oman Sea under the Makran.

Zone 16 represents Alborz and southern area of Sirjan. One part of this zone, nearly south of Sirjan, is not similar to ophiolitic complex and arise from tensile tectonic and uplifting of the mantle (Aghanabati, 2004). In this zone variation range of Bouguer and gravity anomalies is maximum and it is isostatically overcompensated. It almost contains igneous rocks of Paleozoic.

Zone 17 is High Zagros Thrust zone. Its dominant trend is northwest-southeast. It is comparable with Zagros thrust zone of Stocklin (1968). It consists of Mesozoic rocks. Average of elevation, free air and Bouguer anomaly are deterministic features for this zone. These features together with b-value show the active thrust faulting in this zone.

Zone 18 indicates flysch and ophiolities of Makran that is characteristic of the active margin. This zone is coincident with major transpressional strike-slip systems that form the eastern boundary (Ornah-Nal and Chaman fault zones) and the western boundary (Minab-Zendan-Palami fault zone) of Makran which both of them have responsible for several destructive earthquakes. The value of seismic energy released in this zone is maximum that is evidence for seismicity of this zone.

Zone 19 demonstrates Simple Folded Belt of Zagros and approximately is correlated by Foothill folded series of Nowroozi (1976). The characteristic of this zone is the frequency of earthquakes greater than m_c. Based on maximum elevation it is situated after zone 17. Average of free air anomaly and minimum of isostasy are the other important feature of this zone that enforce on shortening of the crust due to the collision in this region. This zone is composed of sedimentary rocks.

By taking into consideration of Fig. 8, it is illustrated that the result of SOM has been led to a good identification of tectonic zones in Iran. Some zones in our new approach are comparable to those in conventional

map but there aren't exactly the same. For example Urumiyeh-Dokhtar (zone 1), Lut and Great Kavir (zone 3), Sanandaj-Neyriz (zone 11), Kopeh-Dagh (zone 12), Arabian platform (zone 14), Makran (zone 15), Alborz (zone 16), High Zagros Thrust zone (zone 17), Simple folded belt of Zagros (zone 19) have their correspondence in conventional map but there are some differences between them, one can compare these zones in Fig. 8 and 1. This is because we have taken into account both surficial and subsurficial features that have not been considered in conventional map.

On the other hand, some regions are detected only in automated tectonic zoning as individual zones, these zones are as: 2, 4, 5, 6, 7, 8, 9, 10, 13 and 18. Besides all of these, together cluster visualization capability of SOM and topology-preserving property of feature map give some other valuable results that have not been previously noticed in tectonic zoning. These important results are based on similarity or dissimilarity between different clusters which is illustrated by U-matrix and feature map (Fig. 7). The interesting ones are: similarity between the Kopet Dagh Ranges in the northeast and the High Zagros thrust zone in the Southwest (zone 12 and zone 17 in Fig. 7a), similarity between Alborz and northern parts of zone 13 (Fig. 7b), similarity between flysch of Makran and High Zagros Thrust zone (neighboring zones 18 and 17 in Fig. 7b), similarity between Bazman and Taftan Volcano and the Ferdows Block (zone 9 and 7 in Fig. 7b) despite of geographical separation and also dissimilarity between Simple Folded Belt and High Zagros thrust zone (zone 19 and zone 17 in Fig. 7b), dissimilarity between Sanandaj metamorphic zone and High Zagros Thrust zone (zone 11 and 17 in Fig. 7b) despite of geographical vicinity. Highlighting the trends of active faults is also another important benefit of SOM. One can compare the location of Main Zagros Thrust, Nayband fault, Neh fault, Sabzevaran fault, Kazerun flexure, Minab fault, Doruneh fault, Gowk fault, Dasht-e-Bayaz fault, … in two Fig. 2 and 8.

There are some similarities between numerical tectonic maps and conventional maps. One of the most distinctive properties of this numerical method is that geographically separated areas are detected as homogenous zones if they have similar tectonic characteristics and vice versa, unified regions are separated based on different tectonic characteristics. However, understanding similarities according to applied variables needs further analysis which was not included here.

It is important to recognize that tectonic zones generated by SOM are purely based on the geophysical and geological attributes presented in Table 1. So, correspondences and differences between the automated tectonic zones based on SOM and given zones based on conventional method must receive careful thought.

At last, this method can be applied in regions where their tectonic regionalization is not well known.

CONCLUSIONS

In this study, we used the clustering and visualization capabilities of self-organizing map neural network for analyzing high-dimensional geological and geophysical data in order to quantitative tectonic zoning. SOM were used because the implement the orderly mapping of a high-dimensional distribution onto a regular low-dimensional grid and are thereby able to covert complex nonlinear statistical relationships between high-dimensional geological and geophysical data items into simple geometric relationships on a low-dimensional display.

In this study, all presently available information including digital geological maps of the Geological Society of Iran, geological maps of the National Iranian Oil Company (NIOC), Tectonics map of Iran, Magnetic total intensity maps of Iran, geophysical map of Iran, geophysical data, earthquake events reported from ISC, PDE, USGS sites and other manual source from 1900 till 2008 were used as input data. However, the work is preliminary subject to future changes as new information is provided or new data collected.

The SOM not only have capability in clustering but also visualization utility of SOM can help us to well interpret of tectonic zones and tectonic features. The component planes constructed here by SOM were successful in determining parameters for distinguishing the different tectonic zones. Component planes helped to determine the relationships between variables and their distribution in tectonic zones. Based on these planes, we modified the variables to attain better clustering. U-matrix can also reveal statistical distribution of high-dimensional geological and geophysical data into a two-dimensional map. Similarity and dissimilarity between some specific zones can be distinguished by feature map that haven't been noticed previously.

One of the most distinctive properties of this numerical method is that geographically separated areas are detected as homogenous zones if they have similar tectonic characteristics and vice versa, unified regions are separated based on differentiation of their tectonic characteristics.

The SOM is therefore very suitable for tectonic zoning especially in regions where their tectonic regionalization is not well known.

ACKNOWLEDGMENTS

This study was supported by the center of Excellence for Environmental Geohazrads and the Research Council of Shiraz University. We appreciate Mr. Maghareh and Mr. Kazimipour for supplying some basic codes from SOMToolbox.

REFERENCES

Aghanabati, A., 1986. Geological Map of the Middle East. Published Geological Survey of Iran, Iran.

Aghanabati, A., 2004. Geology of Iran. Geological Survey of Iran Publ., Tehran, ISBN: 964-6178-13-8, pp: 586.

Alavi, M., 1994. Tectonic of the zagros orogenic belt of Iran: New data and interpretations. Tectonophysics, 229: 211-238.

Ambraseys, N.N. and C.P. Melville, 1982. A History of Persian Earthquakes. Cambridge University Press, Cambridge, pp: 219.

Axen, G.J., P.S. Lam, M. Grove, D.F. Stockli and J. Hassanzadeh, 2001. Exhumation of the west central Alborz Mountains, Iran, Caspian subsidence and collision-related tectonics. Geology, 29: 559-562.

Berberian, M., 1981. Active Faulting and Tectonics of Iran. In: Zagros-HinduKush-Himalaya Geodynamic Evolution, Gupta, H.K. and F.M. Delaney (Eds.). American Geographical Union, Washington, DC., pp: 33-69.

Berberian, M. and G.C.P. King, 1981. Towards a paleogeography and tectonic evolution of Iran. Can. J. Earth Sci., 18: 210-265.

Berthold, M. and D.J. Hand, 1999. Intelligent Data Analysis: An Introduction. 1st Edn., Springer, USA., ISBN: 3-540-65808-4.

Boulin, J., 1991. Structures in Southwest Asia and evolution of the Eastern Tethys. Tectonophysics, 196: 211-268.

Choubert, G. and A.M. Faure-Muret, 1980. Geological World Atlas, Sheets 9, 10 and 11 (1/10,000,000). In: Commission for the Geological Map of the World, Dijon, R. (Ed.). UNESCO, Paris.

Davies, D.L. and D.W. Bouldin, 1979. A cluster separation measure. IEEE. Trans. Pattern Anal. Mach. Intel., 1: 224-227.

Davoudzadeh, M., G. Lensch and K. Weber-Diefenbach, 1986. Contribution to the paleogeography, stratigraphy and tectonics of the Infracambrian and Lower Paleozoic of Iran. Neues Jahrbuch Fuer Geol. Palaontol., 172: 245-269.

Davoudzadeh, M. and K. Weber-Diefenbach, 1987. Contribution to the paleogeography, stratigraphy and tectonics of the Upper Paleozoic of Iran. Neues Jahrbuch Fuer Geologie und Palaontologie, 175: 121-145.

Dehghani, G.A. and J. Makris, 1983. The gravity field and crustal structure of Iran. Geodynamic Project (Geotraverse) in Iran, Geological Survey of Iran, Report No. 51, pp: 51-68.

Eftekharnezhad, J., 1980. Subdivision of Iran into different structural realms with relation to sedimentary basins. Bull. Iran. Petroleum Inst., 82: 19-28, (In Farsi).

Eftekharnezhad, J. and A. Behroozi, 1991. Geodynamic significance of recent discoveries of ophiolites and late paleozoic rocks in NE-Iran (Including Kopet Dagh). J. Geosciences Geol. Survey Iran, 1: 4-15.

Engdahl, E.R., J. Jackson, S.C. Myers, E.A. Bergman and K. Priestley, 2006. Relocation and assessment of seismicity in the Iran region. Geophys. J. Int., 167: 761-778.

Fayyad, U., G. Piatetsky-Shapir and P. Smyth, 1996. Knowledge discovery and data mining: Towards a unifying framework. Proceeding of the 2nd International Conference on Knowledge Discovery and Data Mining, (KDDM' 96), AAAI Press, Portland, OR, pp: 82-88.

Gordon, A.D., 1999. Classification. Chapman and Hall, London, ISBN: 1584880139, pp: 417.

Gutenberg, B. and C.F. Richter, 1954. Seismicity of the Earth and its Associate Phenomena. Princeton University Press, Princeton, New Jersey, pp: 310.

Hand, D., H. Mannila and P. Smyth, 2001. Principles of Data Mining. MIT Press, Cambridge, MA.

Hewitson, B.C. and R.G. Crane, 1994. Neural Nets: Applications in Geography. Kluwer Academic Publishers, London.

Hewitson, B.C. and R.G. Crane, 2002. Self-organizing maps: Applications to synoptic climatology. Climate Res., 22: 13-26.

Jackson, J. and D. McKenzie, 1984. Active tectonics of the Alpine-Himalayan belt between Western Turkey and Pakistan. Geophys. J. Royal Astronom. Soc., 77: 185-264.

Jackson, J. and D. McKenzie, 1988. The relationship between plate motions and seismic moment tensors and the rates of active deformation in the Mediterranean and Middle East. Geophys. J., 93: 45-73.

Karakaisis, G.F., 1994. Long-term earthquake prediction in Iran based on the time-and magnitude-predictable model. Phys. Earth Planet. Interiors, 83: 129-145.

Kaski, S., J. Kangas and T. Kohonen, 1998. Bibliography of self-organizing map (SOM) papers: 1981-1997. Neural Comp. Surv., 1: 102-350.

Kohonen, T., 1982. Self-organized formation of topologically correct feature maps. Biol. Cybernet., 43: 59-69.

Kohonen, T., 1984. Self-Organization and Associative Memory. Springer Verlag, Berlin.

Kohonen, T., 1997. Self-Organizing Maps. Springer, New York.

Kraaijveld, M.A., J. Mao and A.K. Jain, 1995. A nonlinear projection method based on Kohonen's topology preserving maps. IEEE Trans. Neural Networks, 6: 548-559.

McCall, G.J.H., 1996. The inner Mesozoic to Eocene ocean of south and central of Iran and associated microcontinents. Geotectonics, 29: 490-499.

Meyer, B. and K. Le-Dortz, 2007. Strike slip kinematics in Central and Eastern Iran: Estimating fault slip-rate averaged over the Holocene. Tectonics, 26: TC5009-TC5009.

Nabavi, M.H., 1976. An introduction to the Iranian geology. Geological Survey of Iran, Report No. 38, pp: 110, (In Farsi).

Nowroozi, A.A., 1971. Seismotectonics of the persian plateau, eastern turkey, caucasus and Hindu-kush regions. Bull. Seismol. Soc. Am., 61: 317-341.

Nowroozi, A.A., 1976. Seismotectonic provinces of Iran. Bull. Seismol. Soc. Am., 66: 1249-1276.

Nowroozi, A.A., 1979. Berberian: Comparison between instrumental and macroseismic epicenters. Bull. Seismol. Soc. Am., 69: 641-649.

Rieben, H., 1955. The geology of the Tehran plain. Am. J. Sci., 253: 617-639.

Shoja-Taheri, J. and M. Niazi, 1981. Seismicity of the Iranian Plateau and bordering regions. Bull. Seismol. Soc. Am., 71: 477-489.

Stahl, A.F., 1911. Zur geologie von persien. Handbuch der Regionalen Geologie, Band 5, Heft 8, Heidelberg, Germany, pp: 46.

Stocklin, J., 1968. Structural history and tectonics of Iran: A review. Bull. Am. Assoc. Petroleum Geol., 52: 1229-1258.

Stocklin, J. and M.H. Nabavi, 1973. Tectonic map of Iran (1/2,500,000). Ministry of Mines and Metals, Geological Survey of Iran.

Takin, M., 1972. Iranian geology and continental drift in the Middle East. Nature, 235: 147-150.

Ultsch, A. and H.P. Siemon, 1990. Kohonen's self organizing feature maps for exploratory data analysis. Proceedings of the International Neural Network Conference, (INNC'90), Dordrecht, Netherlands, Kluwer, pp: 305-308.

Venna, J. and S. Kaski, 2001. Neighborhood preservation in nonlinear projection methods: An experimental study. Proceedings of International Conference on Artificial Neural Networks, Aug. 21-25, Springer-Verlag, London, UK., pp: 485-491.

Vesanto, J. and J. Ahola, 1999. Hunting for correlations in data using the self-organizing map. Proceeding of the International ICSC Congress on Computational Intelligence Methods and Applications, Jun. 22-25, ICSC Academic Press, New York, USA., pp: 279-285.

Vesanto, J., 2002. Data exploration process based on the self-organizing map. Ph.D. Thesis, Helsinki University of Technology, Acta Polytechnica Scandinavica, Mathematics and Computing Series No. 115, pp: 96.

Walker, R. and J. Jackson, 2002. Offset and evolution of the Gowk fault, S.E. Iran: A major intra-continental strike-slip system. J. Struct. Geol., 24: 1677-1698.

Zamani, A. and N. Hashemi, 2000. A comparison between seismicity, topographic relief and gravity anomalies of the Iranian Plateau. Tectonophysics, 327: 25-36.

Zamani, A. and N. Hashemi, 2004. Computer-based self-organized tectonic zoning: A tentative pattern recognition for Iran. Comput. Geosci., 30: 705-718.